Proceedings of the 1996 IEEE
International Conference on Robotics and Automation
Minneapolis, Minnesota - April 1996

A Novel Material Handling System

Tanya J. Snyder and H. Kazerooni
Mechanical Engineering Department
University of California, Berkeley CA 94720

1. Introduction

It is estimated that US industry spends more than $16 billion per year on back injury related costs such as down time and workman's compensation. As a result, industries in which back injuries often occur have some interest in finding a solution to this problem. Such industries include heavy machinery manufacture and assembly, warehousing, package delivery, luggage loading/unloading, and nursing.

To address this problem, a robotic material handling system has been designed and constructed at UC Berkeley shown in Figure 1 . The machine, which has two arms and two legs, operates by following an operator's natural movements, and at the same time augmenting his/her load carrying ability. It is expected that such a machine will significantly reduce the risk of lower back injury due to the fatigue and stress of frequent lifting. A control architecture for the arms has been implemented, while a stable walking control structure is still under development. Section 2 provides background related to this system. In Section 3, system mechanical and electrical hardware hardware are presented. Section 4 gives models for the material handling system arms, the human operator's arms, and the environment. A control architecture for the arms subsystem is developed in section 5, and in sections 6 and 7, force reflection and closed loop stability are discussed.

2. History

The concept of a device which could increase the strength of a human while utilizing the human's intellect for supervisory control has existed since the early 1960s. Originally named a "man-amplifier", the device was first conceived as a master-slave manipulator system.

In the early 1960s, the Department of Defense was interested in developing a powered "suit of armor" to augment the lifting and carrying capabilities of soldiers. The original intent was to develop a system which would allow the human operator to walk and manipulate very heavy objects. In 1964 the Cornell Cornell Aeronautical Laboratory developed a preliminary arm and shoulder design. This design demonstrated that the amplifying ability of the manipulator was limited by the physical size of the hydraulic actuators required to amplify the human operator's strength [9, 10, 11].

From 1966 to 1971, General Electric completed work on the man-amplifier concept through prototype development and testing. This man-amplifier, known as Hardiman, was a system of two overlapping exoskeletons worn by the human operator. The inner exoskeleton was a master manipulated by the human, and the hydraulically-actuated outer exoskeleton was the slave [2, 3, 4].

The robotic material handling system discussed here differs from that of a master-slave system in that a single mechanical manipulator is worn directly by the operator, and command signals are generated naturally by contact forces between the operator and the machine. Through that contact, the operator also receives force information associated with the behavior of the load [5, 6, 7].

The objective of the project presented in this paper has been to design and construct a multi-degree of freedom mobile system which could be used for general purpose material handling.

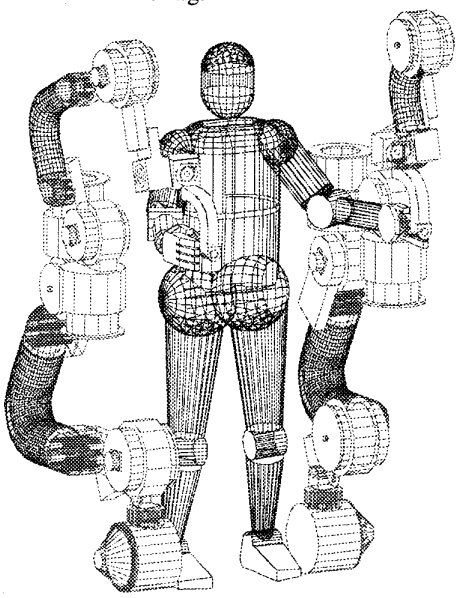

Figure 1. Robotic Material Handling System

3. Hardware

Mechanical Hardware

The system is composed of two arms and two legs, as shown in the schematic diagram of Figure 1. The arm and leg subsystems are intended to be joined through a composite link referred to as a back panel. To verify performance of each subsystem prior to coordination of

the entire machine, the arms and legs have been built separately, as shown in Figures 2 and 3.

Each arm has five serial joints. An additional "false" degree of freedom exists between the operator's hand and the machine, allowing the operator arbitrary control of his/her hand position and orientation within the allowable work envelope. The first three arm joints are powered by actuators which will be described below.

The wrist of the machine is comprised of the remaining two joints, and the "false" degree of freedom previously mentioned. A molded rubber hand piece

Figure 2. Material Handling System Arms

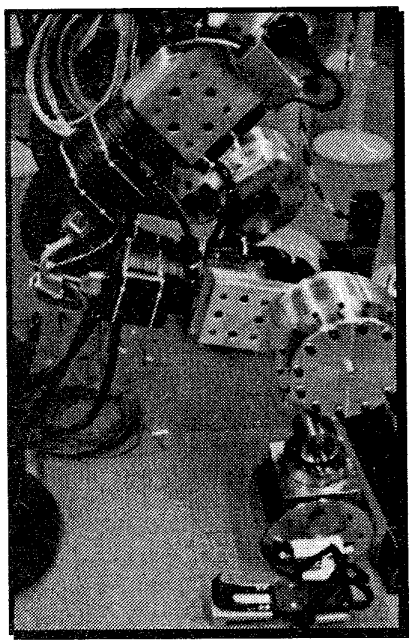

Figure 3. Material Handling System Legs

serves as the interface between the operator and the machine. The wrist joints are unpowered and are arranged in a spherical configuration with the handpiece at the center of their axes. The consequence of this feature is that positioning of a load is accomplished by actuation of the first three powered joints, while orientation of the end effector is achieved through wrist motions powered by the operator. The wrist has been designed to have a degenerate configuration for all possible orientations of the wrist in the targeted work envelope. Such an architecture insures that any loads applied to the end effector will not manifest themselves in moments which must be supported by the operator.

In between the elbow and the wrist are two mechanisms for adjustment of the position and orientation of the wrist relative to the rest of the arm. These adjustment mechanisms are included to explore issues of comfort, and are essentially joints that are locked in place during machine operation. A three axis piezoelectric force sensor is mounted in between the rubber hand piece and the end effector.

Each leg has four serial degrees of freedom, and in this case, three additional "false" degrees of freedom are used in the interface between the operator and the machine. Similar to the those of the arm, the upper three leg joints are powered.

To avoid the use of a long "foot" to support torque at the "ankle" of the machine, there are not any actuators beyond the knee; the final degree of freedom for the leg is the rolling contact that occurs between the ankle and the ground. At the ankle, rotary and linear bearings provide degrees of freedom which are intended to isolate a foot pedal to which the operator's foot is connected through a bicycle cleat. This cleat further allows for rotary motion of the foot from side to side. In between the knee and the ankle are two additional adjustment mechanisms, similar to those of the arms, which alter the position and orientation of the ankle relative to the rest of the leg. A three axis force sensor is mounted in between the foot pedal and the ankle bearing assembly.

The links used in the arms and legs have been constructed from a carbon-composite material formed around a structural foam core. Aluminum inserts bonded to the composite links are used for connecting each link end to its corresponding actuator. The links are curved so as to avoid interference with the operator and the rest of the machine during operation.

Electrical/Control Hardware

Control of the system is carried out through the use of two personal computers equipped with various I/O boards. One computer is used for arm control, and one for leg control. No communication is necessary between the two computers, since motion coordination of the arms and legs occurs naturally through the human/machine interface. The control hardware for the arms is shown in Figure 4. Leg control hardware is virtually identical to that of the arms.

4. Modeling

This section models the dynamic behavior of the robotic material handling arm, the human arm, and the environment. Unstructured models are used. Although a fairly accurate model of the machine and environment can be developed, derivation of a model of the human arm dynamic behavior is rather difficult because of variations in human arm impedances. While this unstructured approach does not lead to any particular controller design, it does lead to an understanding of the fundamental issues involved in control of the machine.

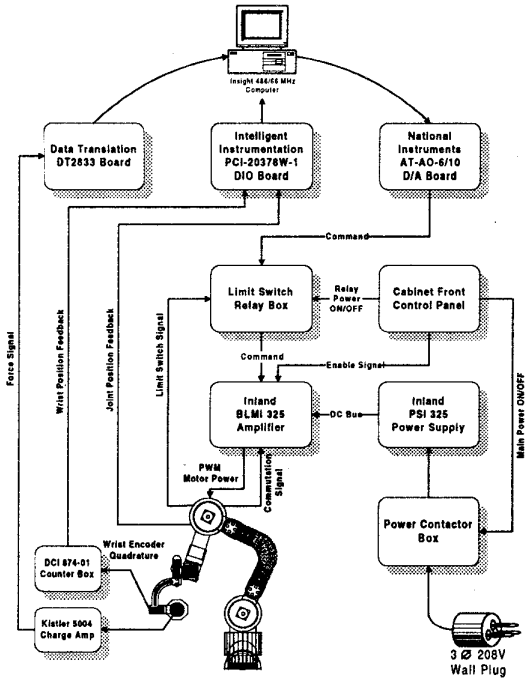

Figure 4: Overall Configuration of the Arm Electrical/Control Hardware.

Robotic Material Handling Arm Dynamics

Each of the joints of the robotic material handling arms has a closed-loop velocity controller which minimizes the effects of frictional forces in the motor and transmission mechanisms, and leads to a more linear and definite dynamic behavior for each of the joints. This allows the use of transfer functions as an approximate representation for the arm's closed- loop dynamic behavior. Minimizing the effects of uncertainty in electromechanical systems is a common design specification for closed-loop controllers. (See Ref. 12 for a design method.)

The motion of the endpoint of the robotic arm is a function of the inputs to each of its closed-loop actuator systems, e, the forces applied to the machine by the operator f_h, and the forces applied to the machine by the environment, f_e. If G_o is a transfer function mapping the open-loop robotic arm endpoint velocity v to an input, K_v is the velocity compensator around each joint, and S_o is a transfer function mapping the robotic arm endpoint velocity v to the forces f when the velocity loop is not closed, then the closed-loop velocity control system is as shown in Figure 5. If we call

$$G_{cl} = \frac{G_o K_v}{1 + G_o K_v} \quad (1) \quad \text{and} \quad S_{cl} = \frac{S_o}{1 + G_o K_v} \quad (2)$$

it can be seen that the endpoint dynamic behavior can be expressed by the following equation:

$$v = G_{cl} e + S_{cl}(f_h + f_e). \quad (3)$$

Motion of the machine endpoint in response to the imposed forces f_h and f_e is due to either structural compliance in the machine or the compliance of the closed-loop velocity controllers around each of the joints. The sensitivity function S_{cl} relates the forces due to human and environmental contact to the robot's endpoint velocity. Note that G_{cl} and S_{cl} depend on the nature of

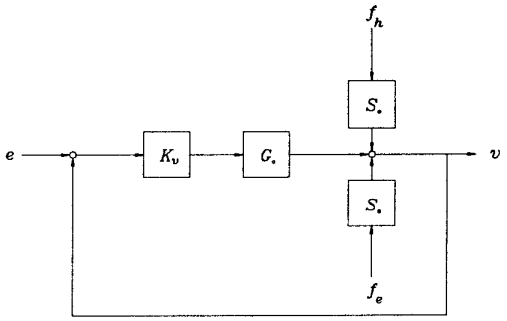

Figure 5: Block diagram of material handling robot with closed-loop velocity controller around each joint.

the closed-loop velocity controller. If a compensator with several integrators is chosen to ensure small steady-state errors, then S_{cl} will be small in comparison to G_{cl}. If the robot's actuators are non-backdriveable, then S_{cl} will be small regardless of the structure of the hand controller's velocity compensator.

Human Arm Dynamics

Human arm maneuvers fall into two categories: constrained and unconstrained. Since the human arm is always holding onto the robotic material handling arm

during a maneuver, the primary focus of this analysis is on constrained maneuvers of the human arm. The dynamic behavior of the human arm's single-joint movements can be modeled as a functional relationship between a set of inputs and a set of outputs. A particular class of dynamic behavior is not assigned to this motion, as it is not clear whether the arm behaves as a force or a position control system in a constrained motion [8]. Rather than attributing a particular control action to constrained movements of the human arm, we use a Norton or Thevenin equivalent concept to arrive at a general substitute for the dynamic behavior of the human arm interacting with the robotic machine. Using the "force-current" analogy between electrical and mechanical systems, a Norton equivalent is chosen to model the human arm's dynamic behavior as a nonideal source of force interacting with the hand controller. The source is considered to be nonideal because the human arm responds not only to commands from the central nervous system, but also to motion constraints imposed by interaction with the robot.

The contact force as commanded by the central nervous system to be imposed by the muscles is denoted as m. If the human arm is not moving, the contact force f_h is equivalent to m. However, if the human arm moves as a result of a motion constraint of the robot, the contact force will differ from m. Considering this, the human contact force f_h can be represented by

$$f_h = m - Hv \qquad (4)$$

where H maps the robot motion constraint onto the contact force. H is referred to as the human arm impedance, and its value is determined primarily by physical and neural properties of the human arm. It will become clear later that H plays an important role in the stability and performance of the system. As mentioned previously, there is a great deal of variation in the value of H; for empirically derived models see Refs. 1 and 13.

Environment Dynamics

The structure of the environment dynamics is similar in form to that of the human arm dynamics in that the forces applied to the robot by the environment are a function of both the load l and the motion of the machine. The environment contact force, f_e can be represented by

$$f_e = l - Ev \qquad (5)$$

where E maps robot motion onto the environmental contact force. E is referred to as the environment impedance.

Figure 6 depicts the dynamic interaction of the robotic material handling arm, the human operator, and the environmental load.

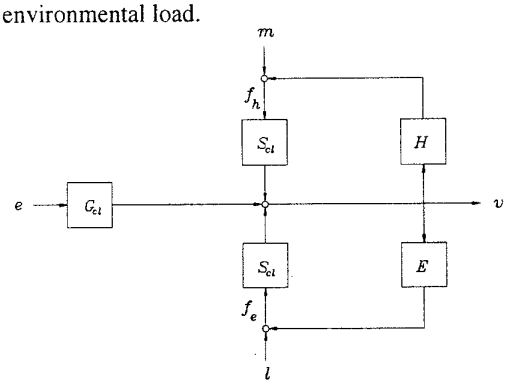

Fig. 6: Block diagram of material handling robot, human arm and environmental load dynamics.

5. Control Architecture

When the material handling robot is not in contact with the operator or the environment, the velocity of the machine's endpoint is governed by Equation 3, where $f_h = 0$ and $f_e = 0$. A feedback loop due to contact force of the operator closes naturally through S_{cl} when the operator holds onto the machine endpiece. Some motion of the machine results through this loop as f_h acts through S_{cl}. However, S_{cl} is generally small in comparison to G_{cl}. Accordingly, some means is necessary to transform the human operator's contact forces into desired motions of the robot (and simultaneously motions of the load). This is accomplished through the incorporation of a force compensator P in the control structure, as shown in Figure 7. To implement this force compsensator, the forces imposed by the operator on the machine are measured by a force sensor, and sent to the controlling microcomputer.

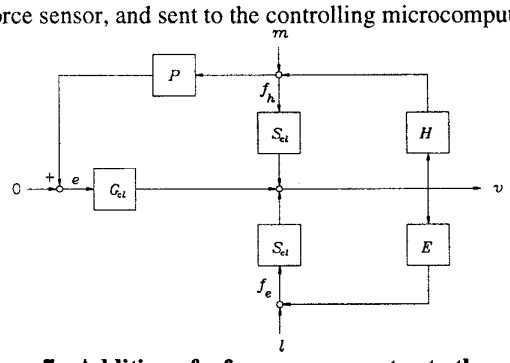

Figure 7: Addition of a force compensator to the control structure.

From Figure 7 it can be seen that P provides an addition path by which the operator's contact forces are mapped onto the endpoint velocity when P is chosen to be

nonzero. The compensator P can be thought of as a component that can be used to shape the overall relationship between the human operator's applied forces f_h and the endpoint velocity v. This leads to an effective sensitivity of $S_{cl} + G_{cl}P$.

The values of G_{cl} and S_{cl} are determined by the mechanical design of the robotic material handling arm and by the chosen closed-loop velocity controllers around each of the arm's joints. The designer does have the freedom to alter the effective sensitivity ($S_{cl} + G_{cl}P$) relating f_h to v by varying P. However, arbitrarily large values cannot be chosen for P, as closed loop stability must also be guaranteed for the system. Changing $S_{cl} + G_{cl}P$ has an effect on how the robotic arm behavior "feels" to the human operator.

6. Force Reflection

One of the features of the robotic material handling system is that is provides the operator with a scaled down version of the forces incurred by the machine itself. This attribute, known as force reflection, gives the operator some sense of the magnitude of the load he/she is maneuvering, and is thought to provide a safer operating environment.

The force reflection ratio of a machine, R_f, is a parameter that indicates the difference in the amount of the force felt by the operator carrying no load and the amount of force felt when the operator is carrying a load. For convenience, the force felt by the operator carrying no load is designated as f_h^o, and the force felt by the operator while carrying a load is designated as f_h^L. The force reflection ratio is then defined here as

$$R_f = \frac{f_h^L - f_h^o}{f_e}. \qquad (6)$$

Examining Figure 7, when f_e = 0 (i.e. there is no load on the system), the force felt by the operator for a given velocity of the system is

$$f_h^o = \frac{v}{(G_{cl} + S_{cl})}. \qquad (7)$$

Similarly, when f_e is nonzero, the force felt by the operator is

$$f_h^L = \frac{v - S_{cl} f_e}{(G_{cl} + S_{cl})}. \qquad (8)$$

Substituting Equations 7 and 8 into Equation 6, and considering that the magnitude of S_{cl} is small relative to $G_{cl}P$ results in a force reflection ratio as follows:

$$R_f \cong \frac{-S_{cl}}{G_{cl}P}. \qquad (9)$$

The above equation shows that if the system sensitivity S_{cl} is low, and/or if the closed loop plant G_{cl} or force controller P is large, there will be very little force reflection. On the other hand, if S_{cl} is relatively high, and/or G_{cl} or P are somewhat low, the force reflection ratio becomes rather small.

7. Closed-Loop Stability

It should be noted that there are two natural feedback loops affecting the endpoint velocity v; $S_{cl}H$ represents the feedback loop that occurs as a result of the interaction between the human arm and the robotic arm, and $S_{cl}E$ is the feedback loop mapping the environmental loading contact force onto v. A third feedback loop is also shown in Figure 6.4; $G_{cl}PH$ represents the controlled compliance feedback loop. The Nyquist criterion can be used to obtain a sufficient stability condition when this $G_{cl}PH$ loop is added to the control system [8]. This condition is:

$$\left|G_{cl}P\right| < \left|S_{cl} + \frac{1 + S_{cl}E}{H}\right| \quad \forall\omega \in (0,\infty) \qquad (10)$$

Inequality 10 expresses a stability condition for the closed loop system. Inspection of this equation shows that if the sensitivity S_{cl} is low, and/or if the human arm stiffness H is high, it is necessary to compromise on the magnitude of either P, G_{cl}, or both. Shown in Figure 10 are the effects on system behavior of changes in G_{cl} and P. For methods of improving the stability range, see Ref. 8.

8. Conclusion

In this paper, a novel material handling system has been presented. An overview of the hardware has been provided, and issues related to control of the arms have been discussed. It is believed that when it is completed, use of this material handling system will help reduce or eliminate workplace back injuries due to repetitive lifting.

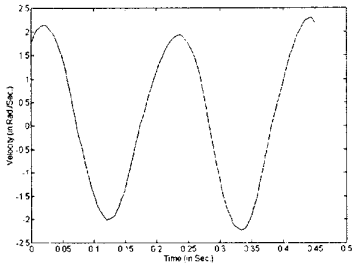

$|G_{cl}|$ low, $|P|$ low

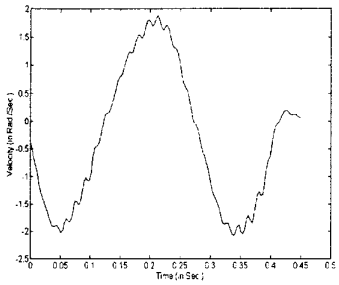

$|G_{cl}|$ high, $|P|$ high

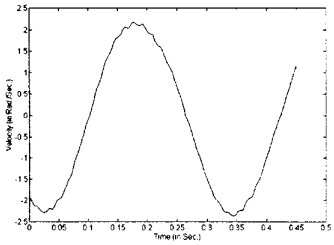

$|G_{cl}|$ low, $|P|$ high

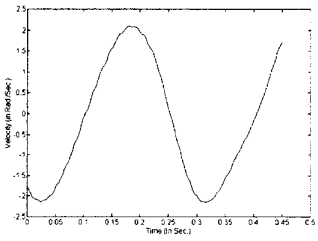

$|G_{cl}|$ high, $|P|$ low

Figure 10: Effects on system behavior with varying controller gain and force gain. Roughness in the curve indicates the onset of instability.

9. References

1. Berthoz, A., Metral, S., "Behavior of Muscular Group Subjected to a Sinusoidal and Trapezoidal Variation of Force", J. of Applied Physiol., Volume 29, pp:378-384, 1970.
2. GE Company, "Exoskeleton Prototype Project, Final Report on Phase I", Report S-67-1011, Schenectady, NY, 66.
3. GE Company, "Hardiman I Prototype Project, Special Interim Study", Report S-68-1060, Schnectady, NY, 1968.
4. Groshaw, P. F., "Hardiman I Arm Test, Hardiman I Prototype", Report S-70-1019, GE Company, Schenectady, NY, 1969.
5. Kazerooni, H., "Human-Robot Interaction via the Transfer of Power and Information Signals", IEEE Transactions on Systems and Cybernetics, Vol. 20, No. 2, Mar. 1990.
6. Kazerooni, H., and Guo, Jenhwa, "Human Extenders", ASME J. of Dynamic Systems, Measurement, and Control, Vol. 115, No. 2(B), June 1993.
7. Kazerooni, H., and Her, M.G., "A Virtual Exercise Machine", Proceedings IEEE International Conference on Robotics and Automation, Vol. 1, pp 238-248, 1993.
8. H. Kazerooni and Tanya J. Snyder, "A Case Study on Dynamics of Haptic Devices: Human Induced Instability in Powered Hand Controllers," AIAA Journal of Guidance, Control, and Dynamics, Feb. 1995, vol. 18 (no. 1), pp 108-113.
9. Mizen, N. J., "Preliminary Design for the Shoulders and Arms of a Powered, Exoskeletal Structure", Cornell Aeronautical Laboratory Report VO-1692-V-4, 1965.
10. Mosher,R.S., "Force Reflecting Electrohydraulic Servomanipulator", Electro-Technology, pp. 138, Dec. 60.
11. Mosher, R. S., " Handyman to Hardiman", SAE Report 670088.
12. Spong, M.W. and Vidyasagar, M., "Robust Nonlinear Control of Robot Manipulators," Proc. 24th IEEE Conference on Decision and Control, Ft. Lauderdate, Florida, pp1767-1772, December 1985.
13. Stein, R. B., "What muscles variables does the nervous system control in limb movements?", J. of the behavioral and brain sciences, Volume 5, pp 535-577, 1982.